Electrical detection of germination of viable model *Bacillus anthracis* spores in microfluidic biochips†‡

Yi-Shao Liu,[a] T. M. Walter,[b] Woo-Jin Chang,[c] Kwan-Seop Lim,[ac] Liju Yang,[d] S. W. Lee,[e] A. Aronson[b] and R. Bashir*[a]

Received 15th February 2007, Accepted 20th March 2007
First published as an Advance Article on the web 5th April 2007
DOI: 10.1039/b702408h

In this paper, we present a new impedance-based method to detect viable spores by electrically detecting their germination in real time within microfluidic biochips. We used *Bacillus anthracis* Sterne spores as the model organism. During germination, the spores release polar and ionic chemicals, such as dipicolinic acid (DPA), calcium ions, phosphate ions, and amino acids, which correspondingly increase the electrical conductivity of the medium in which the spores are suspended. We first present macro-scale measurements demonstrating that the germination of spores can be electrically detected at a concentration of 10^9 spores ml^{-1} in sample volumes of 5 ml, by monitoring changes in the solution conductivity. Germination was induced by introducing an optimized germinant solution consisting of 10 mM L-alanine and 2 mM inosine. We then translated these results to a micro-fluidic biochip, which was a three-layer device: one layer of polydimethylsiloxane (PDMS) with valves, a second layer of PDMS with micro-fluidic channels and chambers, and the third layer with metal electrodes deposited on a pyrex substrate. Dielectrophoresis (DEP) was used to trap and concentrate the spores at the electrodes with greater than 90% efficiency, at a solution flow rate of 0.2 μl min^{-1} with concentration factors between 107–109 spores ml^{-1}, from sample volumes of 1–5 μl. The spores were captured by DEP in deionized water within 1 min (total volume used ranged from 0.02 μl to 0.2 μl), and then germinant solution was introduced to the flow stream. The detection sensitivity was demonstrated to be as low as about a hundred spores in 0.1 nl, which is equivalent to a macroscale detection limit of approximately 10^9 spores ml^{-1}. We believe that this is the first demonstration of this application in microfluidic and BioMEMS devices.

Introduction

Bacillus anthracis has long been identified as the causative agent of the disease anthrax. Like all members of the genus *Bacillus*, it has a long-term environmental persistence due to the formation of endospores, which develop over a time course of several hours inside a cell exposed to nutrient starvation or other environmental stresses.[1] The spores are released to the environment when the cell lyses. A dense protein coat, low cytoplasmal water activity and small, acid soluble DNA binding proteins render the spore highly resistant to dessication, irradiation, chemical oxidation and other environmental assaults.[2] This resistance makes decontamination of an environment in which endospores are present very difficult, and makes detection of low-level spore contamination an important goal.

The binding of certain small molecules to receptors in the spore cytoplasmic membrane initiates an irreversible cascade of events leading to germination of the spore and resumption of vegetative growth.[3–5] Spores from different species of *Bacillus* respond to different germinants, depending on which membrane-bound receptors they express. For example, *B. subtilis* spores germinate in response to L-alanine binding to the receptor GerA,[6] *B. cereus* spores in response to inosine binding to GerI,[7] and *B. megaterium* spores in response to L-proline binding to an undetermined receptor.[8] In some cases, multiple germinants act synergistically at lower concentrations than required for any single germinant,[9] and this is probably the case when spores germinate under physiological conditions in a host.[10,11]

During germination, the loosely cross-linked peptidoglycan of the spore cortex is hydrolyzed, and the spore takes up water, Mg^{2+} and K^+ ions, and releases α-dipicolinic acid (DPA) from the core, along with Ca^{2+} and other ions.[12–14] After this release, the spore becomes heat sensitive, and also loses its refractility, becoming dark when viewed by phase contrast

[a]*Birck Nanotechnology Center, Brindley Bioscience Center, School of Electrical and Computer Engineering, Weldon School of Biomedical Engineering, Purdue University, West Lafayette, Indiana, 47907, USA. E-mail: bashir@purdue.edu; Fax: +1-765-494-6441; Tel: +1-765-4966229*
[b]*Department of Biological Sciences, Purdue University, West Lafayette, Indiana, 47907, USA.*
[c]*ERC for Advanced Bioseparation Technology, Inha University, Incheon, 402-751, Korea.*
[d]*Biomanufacturing Research Institute & Technology Enterprise (BRITE), Department of Chemistry, North Carolina Central University, Durham, NC, 27707, USA.*
[e]*Department of Biomedical Engineering, College of Health Science, Yonsei University, Wonju, Gangwondo, 220-710, Korea.*
† The HTML version of this article has been enhanced with colour images.
‡ Electronic supplementary information (ESI) available: Fig. S1, S2 and S3. See DOI: 10.1039/b702408h

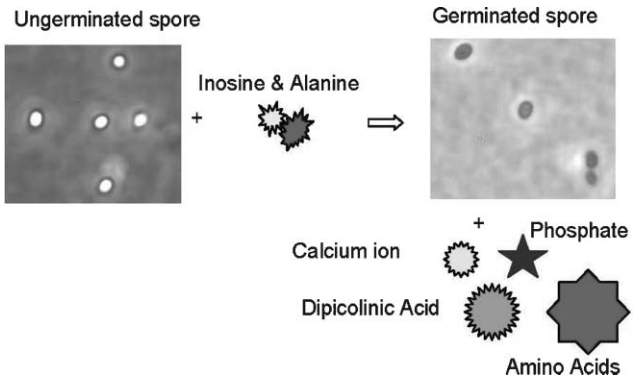

Fig. 1 Rationale for detection of spore germination (magnification: 1000×, DMLB, Leica Microsystems Inc., Bannockburn, IL, USA). Spores begin germination upon addition of the germinant solution. Germinated spores have released ions and lost refractility, becoming phase grey or phase dark.

microscopy (Fig. 1). Little or no metabolic activity occurs until the spore has germinated (has become phase dark).[1,3,4,13] Within a few hours though, metabolism recommences and the spore outgrows, breaking through the spore coat and emerging as a vegetative cell.

The intentional contamination of seven letters with *B. anthracis* spores in 2001 resulted in 22 cases of anthrax, 5 of which were fatal,[15] and focused attention on the detection of spores of this organism in environmental samples. Many detection methods (colony morphology, staining of the unique poly-D-glutamate capsule, PCR amplification of specific DNA sequences, γ-phage susceptibility testing) require the outgrowth of vegetative cells before testing, and also often require time-consuming manual steps. Several other innovative methods[16–21] reported in recent years can detect endospores at a threshold of about 10^3 spores in a sample. Most of these methods involve micro- or macro-scale PCR analysis, or various forms of optical detection. Automated spore detection systems have used real-time PCR with thermal cycling chambers made from etched and fusion-bonded silicon to carry out the PCR based detection assays for *Bacillus* spp. and *Yersinia* spp.[22] Bioaerosol mass spectrometry for rapid detection of airborne pathogens is another example of an automatic spore detection method.[23] It should be noted that most of the reported methods either perform identification of the spores before spores germinate, and do not distinguish between viable and non-viable spores[17] or detect the growth of the vegetative cells.[16] It would be very useful to determine, using automated techniques, whether the spores are indeed viable or not.[22,23]

The method presented herein detects viable spores by their germination using electrical methods. We used *B. anthracis* Sterne endospores as the model organism. The detection mechanism is based on changes in conductivity due to the release of Ca^{2+}, DPA and other ions from the spore cortex upon germination.[13,14,24,25] These charged entities and ions will result in an increase in conductivity of the solution, which can be measured with a commercial conductivity meter, or the embedded electrodes within a microfluidic biochip where the spores are captured. Detection of the released Ca^{2+} and DPA from hydrolyzed endospores has been reported;[25–29] however, none of these methods use automated electrical detection.

Various types of microfluidic biochips have been developed and utilized in applications related to bacterial cell growth and detection. In the recent past, we have developed a silicon-based microfluidic biochip with an anodically bonded glass cover for detecting bacterial metabolism.[30–32] *Listeria monocytogenes* were incubated and metabolic products were electrically detected within just a few hours. Micro-culture systems for continuous observation of physical properties of *Escherichia coli* have recently been reported for examining bacterial quorum sensing and feedback mechanisms.[33,34] Numerous other reports of microfluidic devices related to detection of microorganisms can be found. Nucleic acid based assays have been implemented on-chip using micro-fluidic devices, such as on-chip conventional and real-time PCR,[35,36] and electrochemical detection of the products of PCR, using a poly-TTCA modified screen-printed carbon electrode—allowing the detection of the catalytic oxidation of dsDNA.[37] To the best of our knowledge, electrically based detection of spore germination using microfluidic devices has never been reported.

The proposed detection mechanism, together with innovative BioMEMS fabrication techniques, potentially allows the detection system to be automated, portable, and useful for examining potentially spore-containing samples in industrial microbiology, diagnostics, and environmental surveillance. Most importantly, the proposed approach can be used to determine viability of the spores, in conjunction with PCR or other techniques, which can then be used for the identification of the spore samples.

Materials and methods

Preparation of spores

Spores were prepared by the method of Ireland and Hanna.[38] Briefly, a single colony was inoculated into 50 ml of 2X BHI with 0.5% glycerol and grown overnight at 37 °C. The overnight culture was diluted into 500 ml of CCY medium,[39] and grown at 37 °C with vigorous aeration for 2 to 3 days. The culture was examined by phase contrast microscopy. If it contained >95% phase bright endospores, the spores were harvested by centrifugation for 30 min at 1500 × *g*. The pellet was washed 3 times with 10 volumes of sterile deionized water and resuspended in 4 ml of a 2% aqueous solution of Renografin-76 (ER Squibb & Sons).

Harvested spores were purified by layering onto 30 ml of a 50% solution of Renografin-76 and centrifuging at 12 000 × *g* for 30 min.[40] The pellet was washed 5 times in 2 volumes of deionized water, removing the top flocculent layer after each wash. It was finally resuspended in 2 ml of deionized water. Spores were titered using a Petroff–Hausser chamber and stored at a titer of $>10^{11}$ spores ml^{-1} at 4 °C.

Spore germination

Bacillus spore germination requires binding of germinant to receptors on the spore membrane. Germination depends on the presence of these receptors, which depends in part on the medium in which the spores were prepared.[41] The choice of

germinant, then, is not a routine matter. Whereas physiological concentrations of L-alanine will initiate germination of many *Bacillus* spores, this is insufficient for germination of *B. anthracis* spores. L-Alanine at a concentration of 100 mM has been reported to allow *B. anthracis* germination,[42] but the background electrical conductivity of this solution is too high to detect the release of ions, such as Ca–DPA, from endospores. The purine nucleoside inosine has been reported as a potent germinant of *B. cereus*,[7] but it does not germinate *B. anthracis* spores unless certain amino acids are present as cogerminants.[38] Inosine also has high background conductivity. The best germinant in the present experiment is one that allows substantial spore germination without having a high background electrical conductivity. It was found that a solution of 10 mM L-alanine and 2 mM inosine (Sigma Chemical Corp.) was optimal. The background conductivity was about 20 μS cm^{-1}, and addition to heat-treated spores (65 °C for 30 min) resulted in >75% germination within 20 min. Addition of 1 mM histidine[43] or 10 mM glucose to this solution did not substantially improve germination.

Verification of germination detection using commercial equipment: macro-scale experiment

It is very well known that Ca^{2+} ions, DPA, and other polar and charged entities stored in the endospore cortex, are released when spores germinate.[12–14,24,25] Among these chemical entities, reported DPA content varies and accounts for 5–14% of the total mass of the endospore.[14,24] The release of either Ca^{2+} ions and DPA, or other ions, will contribute to an increase of conductivity in the solution in which the spores germinate. By monitoring the conductivity change of the spore solution, it can be determined whether the captured spores have germinated or not.

The macro-scale experiments measured germination of a 5 ml spore suspension, with concentration ranging from 10^7–10^9 spores ml^{-1}, in a rinsed (sterile deionized water), sterile 15 ml plastic centrifuge tube (Corning 430052) using a commercial conductivity meter (6307 microcomputer pH/conductivity meter, Jenco instrument corp.). The spores were preheated in a 65 °C water bath for 30 min before the experiment started. After spores were heated and germinant solution was added, the conductivity probe was inserted into the 15 ml centrifuge tube containing the sample. Conductivity values were recorded every 1 min. Three different concentrations of spores were compared to control experiments (*i.e.* spores only, deionized water only and germinant only), to find the detection limit. The conductivity probes were calibrated before each experiment. The deionized water had a measured conductivity of 2–3 μS cm^{-1}, which was within the accepted range and thus demonstrated the sensitivity of the instrument. The experiment was carried out at room temperature.[42] The experimental set-up is depicted in Fig. 2. Results are presented below.

Microfluidic device design, fabrication and assembly

As a result of macro-scale experiments that we did to verify the concept of electrical detection of spore germination, several criteria were considered in the design and fabrication of our BioMEMS device: (1) The chip needed to be designed to detect as few spores as possible, but at the same time allow a concentration of about 10^9 spores ml^{-1} to achieve significant signal strength. (2) Separate inlets were required to deliver germinant and spores to prevent the heat-treated spores from coming in contact with the germinant before they were captured in the dedicated conductivity measuring chamber. (3) Embedded electrodes were needed to monitor the electrical admittance change of the spore solution upon germination. As a result, the proposed chip contains 0.1 nl chambers, separate inlets for spore and germinant delivery, and interdigitated electrodes. The two inlets merged at a junction immediately in front of the experimental measuring chambers that contained the electrodes.

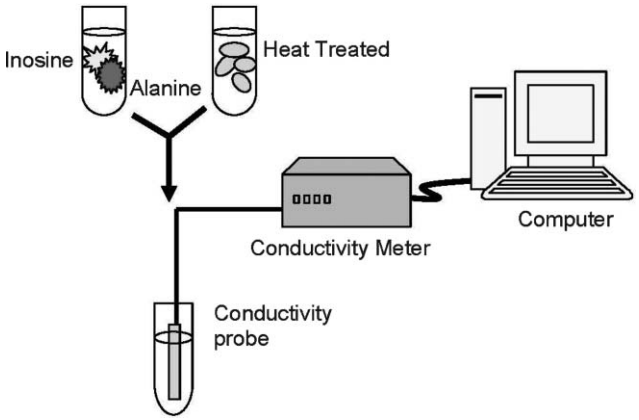

Fig. 2 Schematic of macro-scale experiment, including a commercial conductivity meter (6307 microcomputer pH/conductivity meter, Jenco instrument corp.) and 15 ml tubes (Corning 430052). Spores were activated by preheating to 65 °C for 30 min. Germinant solution (10 mM L-alanine + 2 mM inosine) was added after heat activation. Measurement began immediately upon addition of germinant.

The proposed device was constructed as a three layer BioMEMS device. The first layer was a pyrex (7740, Corning Inc., Corning, NY, USA) substrate with interdigitated electrodes for exerting dielectrophoresis forces to capture spores and for recording the change of admittance within the solution. The metal electrodes were deposited as 250 Å titanium and 350 Å gold by evaporation (CHA e-beam evaporator), followed by a lift-off process. On top of the pyrex substrate was a 40 μm PDMS layer with patterned micro-fluidic channels and chambers. These channels defined the inlet/outlet channels for delivering spores and germinant, and also defined chambers to capture and hold spores for the germination experiment. The third layer was a thick PDMS slab with micro-fluidic pathways serving as valves to close off the channels in the thin second layer. The valving system was designed to enhance the signal strength by forming a closed environment for detection, and also to constrain spores inside the detection chamber after the DEP capture force was released. The use of elastomeric valves made of PDMS has been widely explored.[44] The layout of the chip and the completed chip are illustrated in Fig. 3(a) and (b).

The fabrication of the PDMS layers was done by first preparing SU-8 (MicroChem Corporation, Newton, MA, USA) negative photoresist molds. These molds were made

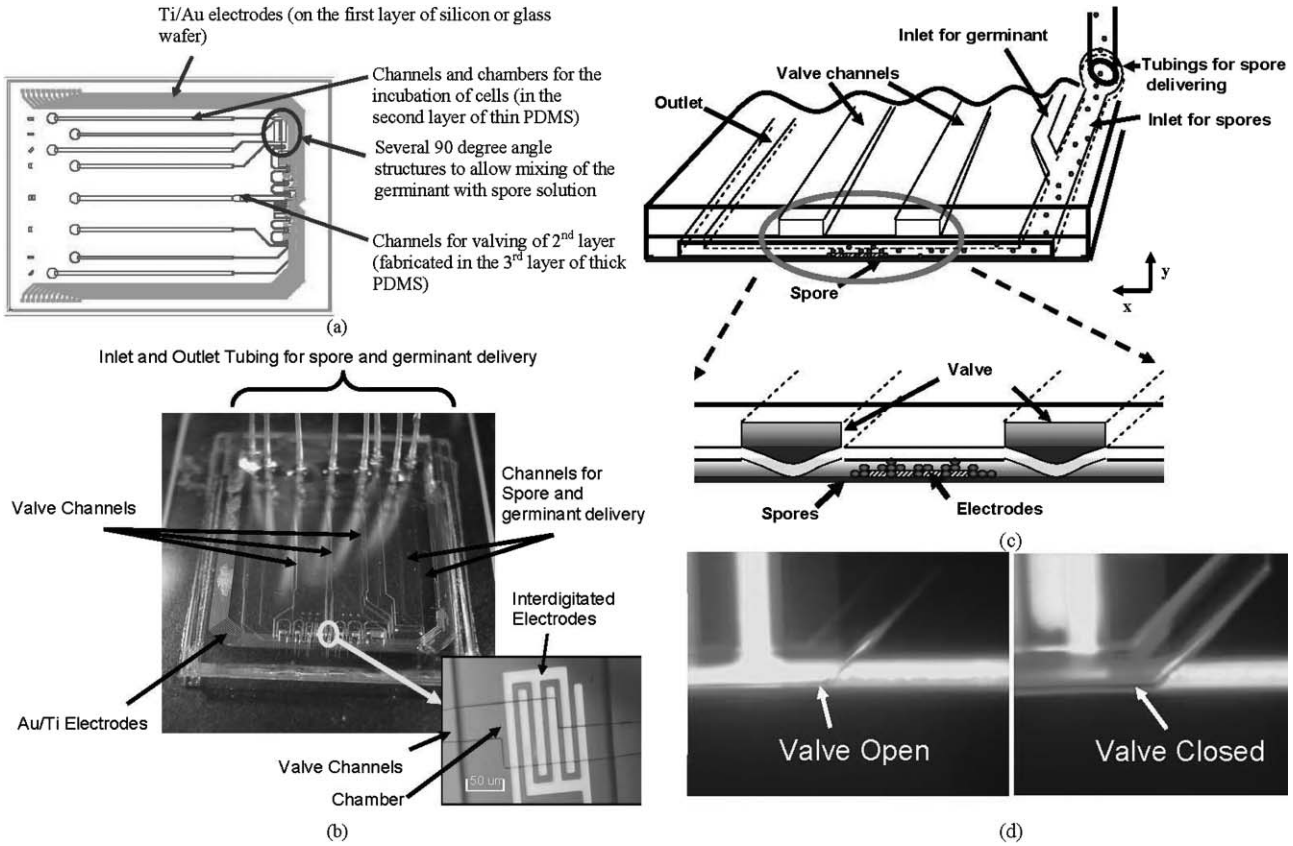

Fig. 3 (a) Drawn top-view layout of the micro-fluidic device, (b) optical image of the completed device, (c) cross-section of the microfluidic device. Spores were heat-activated off-chip, passed through and captured on interdigitated electrodes by DEP in the desired chamber as indicated in Materials and methods. Chambers were filled with germinant (10 mM L-alanine + 2 mM inosine) through fluidic ports. Air valves were actuated by pressurized germinant solution or nitrogen, to isolate spores in dedicated chambers in closed-valve experiments. (d) Valving is effected by pressurizing the third layer and thus pressing against the second layer channel to form a closed environment for spore germination to take place. The effectiveness of the valves was demonstrated with a solution of safranin dye.

with 10 μm features for the second layer and 40 μm features for the third layer by photolithography steps on silicon substrates. A mixture of 30 : 1 (w : w) ratio of elastomer base : curing agent (Sylgard 184 Silicone Elastomer, Dow Corning Corporation, Midland, MI, USA) was thoroughly mixed and spun onto the second layer mold; and a mixture of 3 : 1 (w : w) ratio of elastomer base : curing agent was mixed thoroughly and poured on to the third layer mold. Both PDMS layers were cured in a hard-bake oven at 120 °C for 10 min. The third layer was peeled off after the curing process. Inlet and outlet holes were punched with a punch made from a 22.5 gauge needle. The bonding of the third and the second layers of PDMS was done by visual alignment under a microscope. The two layers were then bonded after curing in a soft-bake oven at 90 °C for 90 min, with the cross-links being formed by the excess elastomer and curing agent on the surfaces between the layers. The inlet/outlet holes of the second layer were then punched with the same punch after the hybrid second–third layer was peeled off of the second layer mold.

PDMS was used for the devices due to its low cost and ease of fabrication. However, concern for leakage of biohazardous substances from PDMS based devices requires care to ensure that the device and surfaces are properly sealed. We also performed all measurements in a biosafety level II hood and ensured that the pressure used for the experiment was less than 30 psi, which is well below the pressure needed to de-bond the PDMS from the pyrex substrate.[45]

The pyrex layer containing the electrode substrate and the hybrid PDMS layer was bonded by surface treatment using oxygen plasma (200 W, 15 s), and aligned immediately (within 5 min). The etch gas was 80% argon and 20% oxygen. Microbore tubings (OD: 0.016 inches, ID: 0.006 inches, Cole–Parmer instrument, Vernon Hills, IL, USA) were inserted into the punched holes and sealed with 10 : 1 PDMS for injection of liquids. The cross-section of the fabricated biochip and how it functions is illustrated in Fig. 3(c) and (d).[32,46,47]

On-chip experiment: spore capture and germination detection

The electrical measurements on-chip were carried out with an automated recording system. The system included an injector, measuring probes (The Micromanipulator Co., Inc. Carson, NV, USA), an LCR meter (Agilent Technologies, Palo Alto, CA, USA), a computer, and a microscope (Eclipse E600FN, Nikon Inc., Melville, NY, USA). Heat treated spores were injected by the injection system into the BioMEMS device mounted on the microscope platform, with a flow rate of 30 μl min^{-1} for 5 min, followed by 0.2 μl min^{-1}. The injection system had multiple injection valves and switches to change

solutions. To avoid contamination, the injection system was located inside a level II biosafety hood and connected to the BioMEMS device with microbore tubing, ferrules, sleeves, and fittings (Upchurch Scientific, Inc., Oak Harbor, WA, USA). The spore samples and germinant solution were prepared and loaded into the system inside the hood. The relatively high initial flow rate (30–35 μl min^{-1}) was used to hasten the delivery from the injection system to the BioMEMS device. With the high flow rate, the injection of solution from inside the hood to the inlets of the chip was done in about 5 min. The flow rate was changed to 0.2 μl min^{-1}, 5 min after injection started. This slower speed guaranteed a spore capture rate of >90% using DEP.[47] The germinant solution was injected after spore capture. Electrical recording started after germinant was delivered into the chip. Data was recorded at 2 min intervals for 1 h. Germinant solution was dyed with safranin to visualize the arrival of germinant into the chip, and also to counter stain *Bacillus anthracis* spores (*i.e.* only the few vegetative cells not removed by the spore purification process will be stained). Verification of germination after each experiment was done by observing the refractility of *Bacillus anthracis* spores using phase contract microscopy. Ungerminated spores are refractile (phase bright) and germinated spores are not (phase grey, or phase dark). The experiment was carried out at room temperature.

Results and discussion

Release of calcium dipicolinic acid

The calcium DPA released during spore germination accounts for most of the increase in conductivity of the spore solution. The amount of DPA in an average *Bacillus subtilis* spore is 4×10^{-16} mole,[48] or 6×10^{-14} g, while the DPA in the largest *Bacillus* spore (*B. megaterium*) is 1×10^{-15} mole (2×10^{-13} g). Assuming 100% release, approximately 10^{-13} g of DPA might be released by a single *B. anthracis* spore upon germination. Therefore, in the germination of 10^9 spores ml^{-1}, we are detecting about 10^{-4} g ml^{-1} increase in DPA ions (and 10^{-5} or 10^{-6} g ml^{-1} for spore concentrations of 10^8 ml^{-1} or 10^7 ml^{-1}, respectively). Assuming 100% DPA release, and that DPA is the major electrically conductive ion released from the spore, release of 10^{-4} g ml^{-1} DPA (100 ppm) would be expected to result in an increase of 150 μS cm^{-1} in conductivity, using the relationship between total dissolved solids (*TDS*) and conductivity: $TDS = k_e EC$, where *TDS* is expressed in mg l^{-1}, k_e is the correlation factor and varies between 0.55 and 0.8, and *EC* is the electrical conductivity in μS cm^{-1} at 25 °C.[49] However, experimental data for the germination of *B. megaterium* spores suggests that only about 700 nanomoles of DPA and Ca^{2+} were released per milligram of spores.[25] That means only about 50% of the expected amount of Ca–DPA is released during germination. Therefore, we might theoretically expect about a 75 μS cm^{-1} increase in conductivity upon germination of 10^9 spores ml^{-1}, based on total dissolved solids.

In fact, in our experiment, the recorded data with different spore concentrations showed that the most significant change of conductivity that we detected was about 10 μS cm^{-1}, which was about 7 times less than we expected; however the measurements are still of the same order of magnitude. Minor experimental error and the known factor that Renografin is a chelator of calcium[50] may have contributed to the lower than expected measurements. It is possible that the rinse and wash steps did not completely remove the Renografin from the surface of the spores, and that as a result the amount of Ca^{2+} released into the solution with the DPA was considerably less than expected.

Detection of spore germination: conductivity based assay at macro scale

The results of spore germination detection with a commercial conductivity meter are illustrated in Fig. 4. This figure shows the results with spore concentrations of 10^7, 10^8, and 10^9 spores ml^{-1}. The most pronounced result is shown at a concentration of 10^9 spores ml^{-1}, where a net increase of conductivity is in the range of 5–7 μS cm^{-1}. An immediate increase in conductivity showed that the germination began in the first 2 min after germinant was added and finished within 20 min, while control experiments showed no significant change in conductivity over time. We regarded the 10^9 spores ml^{-1} as the concentration that can be safely detected, and used this value for design of the micro-scale assay.

Spore germination was verified by phase contrast microscopy (see ESI‡, Fig. S1). Ungerminated spores are phase bright while germinated spores are phase grey, or phase dark. The spores lose their refractility during the germination process.

Spore capture by dielectrophoresis over electrodes embedded on-chip

Spores were delivered to the target chamber (0.1 nl, 100 μm × 100 μm × 10 μm) in a carrier stream of deionized water. The spores were captured at the edge of the embedded electrodes by dielectrophoretic forces induced at 20 V and 100 kHz. With a flow rate of 0.2 μl min^{-1} (peak flow velocity: 40 cm min^{-1}), >90% of the spores in the carrier stream were captured by DEP.[31] We required that DEP forces capture and hold the spores stationary while the water carrier stream was replaced by a stream of germinant solution. A mathematical simulation was performed to help set the

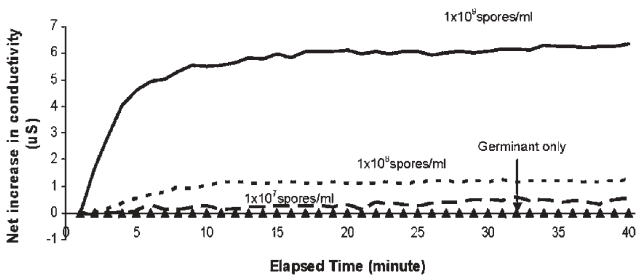

Fig. 4 Results of the macro-scale germination experiment. The graph shows that a concentration of 10^9 spores ml^{-1} has a very clear signal in comparison to the others, while 10^8 spores ml^{-1} is still detectable and 10^7 cells ml^{-1} is too low to be distinguished from the control experiment of germinant solution only.

parameters required for capture, and also to help in the design of the chambers.

The total force[51] acting on a spore suspended in a parabolic laminar flow inside the chamber is given by

$$\vec{F}_{\text{total}} = \vec{F}_{\text{lifting}} + \vec{F}_{\text{sedimentation}} + \vec{F}_{\text{DEP}} + \vec{F}_{\text{drag}} \quad (1)$$

The coordinate system of each force listed above includes a horizontal direction (x-direction) and a vertical direction (y-direction), as shown in Fig. 3(c). The hydrodynamic lifting force,[52] $\vec{F}_{\text{lifting}}$, acting on the spore located on the interdigitated (IDT) electrodes is in the y-direction and the sedimentation force, $\vec{F}_{\text{sedimentation}}$, is in the direction opposite to the hydrodynamic lifting force. At 100 kHz, the Clausis–Mossotti (CM) factor is positive, and the spore is moved toward the region of the largest electric field gradient by the positive dielectrophoretic (DEP) force, $\vec{F}_{\text{DEP}}$, consisting of x- and y-components. The largest electric field gradient is at the edge of the capture electrodes. The y-component of the positive DEP is in the same direction as the sedimentation force. The drag force, $\vec{F}_{\text{drag}}$, is the function of the velocity of the spore.

The DEP force can thus be calculated by the following formula[53,54]

$$\vec{F}_{\text{total}} = \sum_{0}^{\infty} -\nabla U_n \quad (2)$$

where n is the force order, and

$$U_n = -\frac{2\pi\varepsilon_m K_n r^{(2n+1)}}{(2n+1)!!} \sum_{i+j+k=n} \frac{1}{i!j!k!} \left[\frac{\partial^n \Phi}{\partial x^i \partial y^j \partial z^k}\right]^2 \quad (3)$$

where Φ refers to the electrostatic potential of an external electric field and the nth order Clausis–Mossotti (CM) factor is

$$K_n = \frac{n(2n+1)\left(\tilde{\varepsilon}_p - \tilde{\varepsilon}_m\right)}{n\tilde{\varepsilon}_p + (n+1)\tilde{\varepsilon}_m} \quad (4)$$

Simulations of the electric field above interdigitated electrodes with 20 μm width and 8 μm spacing, were performed with the commercially available Finite Element program Ansys (version 5.7, ANSYS Inc.) with grid spacing as small as 0.2 μm. Matlab (R12, The Mathworks) was used to calculate the DEP force, using as input parameters the conductivities and permitivities of DI water and spores,[55] 2.5×10^{-4} S m^{-1}, $78\varepsilon_o$, 5.9×10^{-3} S m^{-1}, and $43\varepsilon_o$, respectively. As a result, the stopping voltage satisfying eqn (1) was about 11.5 V. Therefore, the spore in contact with the electrode should be able to be captured at 20 V which was used for the experiment. The stopping voltage is also exponentially increased as a function of the y-distance between the particle and the electrode (''height''), as shown in ESI‡ Fig. S2. The equilibrium height at which the positive DEP force is equivalent to the drag force is 0.9 μm at 20 V.

Based on this simulation, the DEP forces only extend 0.9 μm above the electrodes in the 10 μm chamber. If the spores were evenly distributed within the flow, we could only capture about 10% of them by DEP. However, considering the gravitational force acting on the spores, most of spores will be flowing at the bottom of the stream when they arrive at the target chamber. Based on the equation governing y-direction movement:

$$\frac{4}{3}\pi r^3(\rho_s - \rho_m)g - 6\pi\mu r u = \frac{4}{3}\pi r^3 \rho_s g \frac{du}{dt} \quad (5)$$

The velocity, u, perpendicular to the flow, and the y-direction displacement, y, can be got from

$$u = \frac{m_d}{k} g\left[1 - \exp\left(\frac{-kt}{m_s g}\right)\right] \quad (6)$$

$$y = \frac{m_d}{k} gt + \frac{m_s m_d g^2}{k^2}\left[\exp\left(\frac{-kt}{m_s g}\right) - 1\right] \quad (7)$$

Thus, with a radius of 0.6 μm, spore width is about 1.2 μm, and if we assume that a spore was at first at top of the channel, the time for it to fall to the bottom of the channel (distance of 10 μm) will be on the scale of 100 s. The horizontal distance traveled in this amount of time will be about 60 cm. Therefore, since the distance from the injection system to the target chambers is about 1 m, the spores are at the bottom of the stream when they approach the capture electrodes. As a result, >90% of spores will be captured at the edges of the electrodes by the DEP forces. Fig. 5 shows the capture of spores by DEP forces, 20 V peak-to-peak, 100 kHz.

Open valve experiment

For the micro-scale experiments, we first germinated the spores without actuating the built-in valve. The spores were captured with DEP forces, and germinant solution was flowed in to replace the deionized water. Measurement of admittance started right after the germinant solution had fully replaced the deionized water. The results showed an increase in admittance upon spore germination (Fig. 6(a)). In comparison to the

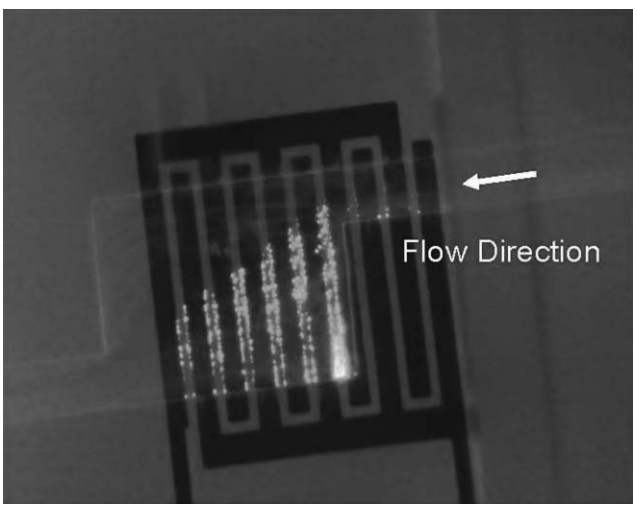

Fig. 5 Fluorescence microscope image of spores captured within the chamber using DEP forces, 20 V peak-to-peak, 100 kHz. Activated spores stained with the FITC dye, $DiOC_6(3)$, were used. Spores were captured primarily at the edges of electrodes, where DEP forces were greatest. Capture occurred first on electrodes closest to the chamber inlet, and subsequently on electrodes further away. Total elapsed time is 1 min.

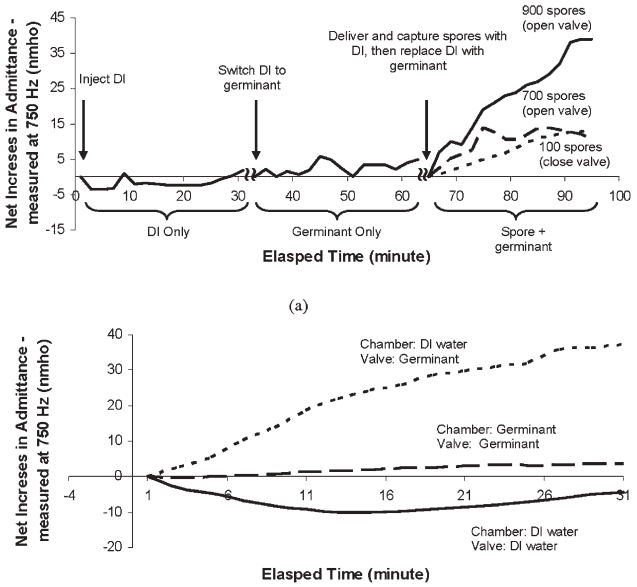

Fig. 6 (a) Representative on-chip experimental results with about 100, 700, and 900 spores in a 0.1 nl chamber (graphs of data with 700 and 900 spores were open valve experiments, while the graph with 100 spores was from a closed valve experiment). The results from serially performed control experiments are also shown. (b) Conductivity changes within the chamber containing different solutions when pressurizing the air channel with different solutions.

control experiment with germinant only, the samples with $\sim$700 spores and $\sim$900 spores presented significant increases in admittance, starting 2 min after the experiment began. There was no significant increase in admittance in the control experiments. Fluctuations in admittance occurred because the chamber was open to the flow stream without the valve actuated. However, when spores started to germinate, enough ions were released to overcome baseline fluctuation and showed a significant increase in admittance. The detection limit with this experiment proved to be a few hundred spores in a 0.1 nl chamber.

Closed valve experiment

To overcome the problem of fluctuations in admittance, we designed a microfluidic valve actuator to isolate the germination chamber from the rest of the system. To actuate the valve, the channels in the third layer of the BioMEMS chip (the PDMS slab) were pressurized with germinant solution to close the valves in the second layer (the PDMS membrane, see Fig. 3(c)). We used germinant solution to close the valves in order to avoid admittance perturbation due to permittivity through the PDMS layer (Fig. 6(b)). It should be noted that we used the germinant solution because if DI water was used, it was observed that the conductivity would change over time, indicating diffusion of the DI water into the measurement chamber. Similarly, if nitrogen gas was used to actuate the valves, gas bubbles were seen to form in the measurement chamber, again indicating the diffusion of gas through the PDMS valve layer into the measurement chamber. Hence the germinant solution was used as the fluid to pressurize the valves. Two sets of measuring probes were used to measure two identical chambers (0.1 nl) simultaneously, with one serving as a control chamber and the other as the experimental chamber. Comparing the results from these two identical chambers, the chamber with spores and germinant had a significant increase in admittance when germination was taking place, whereas the control chamber showed no significant difference from the control experiments without germinant. The sample with 100 spores showed an immediate increase in admittance and reached an admittance increase of $\sim$10 nmho in 20 min. It is clear that only when spore germination was taking place did a significant change in the measured signal occur. (There was a slight admittance increase in the control chamber in the germination experiment due to the influence of ions permeating the PDMS from the experimental chamber.) Comparing the admittance changes with 700 spores in the open-valve experiment and with 100 spores in the close-valve experiment, results were very similar indicating the isolation valves also enhanced the sensitivity of the admittance measurements. This implies that a lower detection limit could be achieved by including isolation valves in the chip design. The detection limit was less than 100 spores in a 0.1 nl chamber (10^9 spores ml^{-1}). Theoretically, this limit could be reduced to 10 spores or even 1 spore with smaller sized chambers.

Delivery of germinant through the PDMS valve actuator

There are several advantages of using PDMS as a fabrication material. It is cheap, biocompatible, easy to make, and transparent, which is good for visual observation, and its elastic property makes the valve structure easy to design. However, PDMS is a porous material and the pore sizes depend on the mix ratio of PDMS base to curing agent. The higher the mix ratio, the less cross-linking, and the softer the cured PDMS is, with more numerous and larger pores. The mix ratio for the second layer of the BioMEMS device was 30 : 1, which is three times higher than the ratio suggested by the manufacturer (Dow Corning Corp.). Therefore, the pressurized germinant solution may penetrate the PDMS membrane into the germination chamber. (Due to this solution permeability, the PDMS must be saturated with water or germinant solution before each experiment.)[32] However, this property also gives us a chance to deliver media to the detection chambers without extra ports or channels. ESI‡ Fig. S3 shows the result of a germination experiment in which germinant solution was introduced to the chamber directly through the valves. The spores were delivered in a stream of deionized water and captured as in other on-chip experiments, except no switch to germinant solution was made. Instead, the third layer valves were actuated with germinant solution. The pressurized germinant solution penetrated through the thin PDMS membrane (30 μm) and entered the germination chamber. Although, not all of the spores germinated this way, we did see (by phase contrast microscopy) that those spores near the valves had germinated (were no longer phase bright).

Conclusion

In this study, we demonstrated a method for automatic and rapid electrical detection of germination of viable spores

within a microfluidic biochip. The biochip includes special design features that facilitate spore capture and electrodes for impedance measurements. The limit of detection was shown to be a few hundred spores in a 0.1 nl chamber, without the use of the isolation valves. The detection limit was reduced to fewer than 100 spores in a 0.1 nl chamber, when the chamber was isolated by closing the isolation valves. The detection limit can be lowered further by using a smaller capture–measurement chamber. The detection time is as short as two hours from heat activation of a suspected organism. Our reported approach can be especially very useful, in combination with other identification methods such as PCR, to rapidly and automatically determine the viability of spores.

Acknowledgements

This work was supported through a grant from NIH R21 AI053683-01 (NIAID) and through a cooperative agreement with the Agricultural Research Service of the United States Department of Agriculture, project number 1935-42000-035. The authors thank Dr Arun K. Bhunia and Dr B. P. Padmapriya for their help with phase contrast microscope imaging. The authors also thank Dr Demir Akin for his help with image recording and analysis. Dr Kwan Seop Lim was supported in part by the Korea Science and Engineering Foundation (KOSEF).

References

1 P. Straiger and R. Losick, *Annu. Rev. Genet.*, 1996, **30**, 297–341.
2 W. L. Nicholson, N. Munakata, G. Horneck, H. J. Melosh and P. Setlow, *Microbiol. Mol. Biol. Rev.*, 2000, **64**, 548–572.
3 P. Setlow, *Curr. Opin. Microbiol.*, 2003, **6**, 550–556.
4 A. Moir, *Annu. Rev. Microbiol.*, 1990, **44**, 531–533.
5 A. Moir, *J. Appl. Microbiol.*, 2006, **101**, 526–530.
6 K. P. McCann, C. Robinson, R. L. Sammons, D. A. Smith and B. M. Corfe, *Lett. Appl. Microbiol.*, 1996, **23**, 290–294.
7 M. O. Clements and A. Moir, *J. Bacteriol.*, 1998, **180**, 6729–6735.
8 D. P. Rossignol and J. C. Vary, *J. Bacteriol.*, 1979, **138**, 431–441.
9 S. Atluri, K. Ragkousi, D. E. Cortezzo and P. Setlow, *J. Bacteriol.*, 2006, **188**, 28–36.
10 P. C. Hanna and J. A. W. Ireland, *Trends Microbiol.*, 1999, **7**, 180–102.
11 J. A. W. Ireland and P. C. Hanna, *Infect. Immun.*, 2002, **70**, 5870–5872.
12 B. M. Swerdlow, B. Setlow and P. Setlow, *J. Bacteriol.*, 1981, **149**, 20–29.
13 P. Setlow in *The Bacterial Spore, vol II*, ed. A. Hurst and G. W. Gould, Academic Press, London, pp. 211–254.
14 M. Paidhungat, B. Setlow, A. Driks and P. Setlow, *J. Bacteriol.*, 2000, **182**, 5505–5512.
15 J. A. Jernigan, D. S. Stephens, D. A. Ashford, C. Omenaca, M. S. Topiel, M. Galbraith, M. Tapper, T. L. Fisk, S. Zaki, T. Popovic, R. F. Meyer, C. P. Quinn, S. A. Harper, S. K. Fridkin, J. J. Sejvar, C. W. Shepard, M. McConnell, J. Guarner, W. -J. Shieh, J. M. Malecki, J. L. Gerberding, J. M. Hughes and B. A. Perkins, and members of the Anthrax Bioterrorism Investigation Team, *Emerg. Infect. Dis.*, **7**, 933–944.
16 H. A. Hartley and A. J. Baeumner, *Anal. Bioanal. Chem.*, 2003, **376**, 319–327.
17 C. Ryu, K. Lee, C. Yoo, W. K. Seong and H. B. Oh, *Microbiol. Immunol.*, 2003, **47**, 693–699.
18 J. Lee and R. A. Deininger, *Luminescence*, 2004, **19**, 209–211.
19 S. L. Welkos, C. K. Cote, K. M. Rea and P. H. Gibbs, *J. Microbiol. Methods*, 2004, **56**, 253–265.
20 T. Hamouda, A. Y. Shih and J. R. Baker, Jr., *Lett. Appl. Microbiol.*, 2002, **34**, 86–90.
21 J. L. Kiel, J. E. Parker, T. R. Grubbs and J. L. Alls, *Chem. Biol. Sens.*, 2000, **4036**, 92–102.
22 B. Hindson, A. Makarewicz, U. Setlur, B. Henderer, M. McBride and J. Dzenitis, *Biosens. Bioelectron.*, 2005, **20**, 1925–1931.
23 *BioAerosol Mass Spectrometry: Reagentless Detection of Individual Airborne Spores and other Bioagent Particles Based on Laser Desorption/Ionization Mass Spectrometry*, report from LLNL, 2004.
24 H. Halvorson and B. Church, *Bacteriol. Rev.*, 1957, **21**, 112–131.
25 I. R. Scott and D. J. Ellar, *J. Bacteriol.*, 1978, **135**, 133–137.
26 M. W. Tabor, J. Macgee and J. W. Holland, *Appl. Environ. Microbiol.*, 1976, **31**, 25–28.
27 A. D. Warth, *Appl. Environ. Microbiol.*, 1979, **38**, 1029–1033.
28 J. F. Powell, *Biochem. J.*, 1953, **54**, 210–211.
29 M. B. Beverly, K. J. Voorhees, R. B. Cody, J. A. Laramée and E. Philips, The 47th ASMS Conference on Mass Spectrometry and Allied Topics, Dallas, TX, 1999, MS-US990609A.
30 R. Gómez-Sjöberg, D. T. Morisette and R. Bashir, *J. Microelectromech. Syst.*, 2005, **14**, 829–838.
31 L. Yang, P. P. Banada, M. R. Chatni, K. S. Lim, A. K. Bhunia, M. Ladisch and R. Bashir, *Lab Chip*, 2006, **6**, 896–905.
32 W. -J. Chang, D. Akin, M. Sedlak, M. R. Ladisch and R. Bashir, *Biomed. Microdev.*, 2003, **5**, 281–290.
33 I. Inoue, Y. Wakamoto, H. Moriguchi, K. Okano and K. Yasuda, *Lab Chip*, 2001, **1**, 50–55.
34 F. K. Balagaddé, L. You, C. L. Hansen, F. H. Arnold and S. R. Quake, *Science*, 2005, **309**, 137–140.
35 E. T. Lagally, J. R. Scherer, R. G. Blazej, N. M. Toriello, B. A. Diep, M. Ramchandani, G. F. Sensabaugh, L. W. Riley and R. A. Mathies, *Anal. Chem.*, 2004, **76**, 3162–3170.
36 E. T. Lagally and R. A. Mathies, *J. Phys. D: Appl. Phys.*, 2004, **37**, R245–R261.
37 M. J. A. Shiddiky, D. S. Park and Y. B. Shim, *Electrophoresis*, 2005, **26**, 4656–4663.
38 J. A. W. Ireland and P. C. Hanna, *J. Bacteriol.*, 2002, **184**, 1296–1303.
39 G. S. A. B. Stewart, K. Johnstone, E. Hagelberg and D. J. Ellar, *Biochem. J.*, 1981, **198**, 101–106.
40 A. O. Henriques, B. W. Beall, K. Rolland and C. P. Moran, Jr., *J. Bacteriol.*, 1995, **177**, 3394–3406.
41 L. M. Hornstra, Y. P. deVries, W. M. deVos and T. Abee, *Appl. Environ. Microbiol.*, 2006, **72**, 3746–3749.
42 R. W. Titball and R. J. Manchee, *J. Appl. Bacteriol.*, 1987, **62**, 269–73.
43 M. A. Weiner, T. D. Read and P. C. Hanna, *J. Bacteriol.*, 2003, **185**, 1462–1464.
44 S. R. Quake and A. Scherer, *Science*, 2000, **290**, 1536–1540.
45 S. Bhattacharya, A. Datta, J. M. Berg and S. Gangopadhyay, *J. Microelectromech. Syst.*, 2005, **14**, 1–9.
46 M. Agirregabiria, F. J. Blanco, J. Berganzo, M. T. Arroyo, A. Fullanondo, K. Mayora and J. M. Ruano-López, *Lab Chip*, 2005, **5**, 545–552.
47 J. Y. Baek, J. Y. Park, J. I. Ju, T. S. Lee and S. H. Lee, *J. Micromech. Microeng.*, 2005, **15**, 1015–1020.
48 A. A. Hindle and E. A. Hall, *Analyst*, 1999, **124**, 1599–604.
49 J. W. Lloyd, and J. A. Heathcote, *Natural Inorganic Hydrochemistry in Relation to Groundwater*, Clarendon Press, Oxford, England, 1985.
50 K. R. Thompson, M. R. Violante, T. Kenyon and H. W. Fischer, *Invest. Radiol.*, 1978, **13**, 238–240.
51 H. Li, Y. Zheng, D. Akin and R. Bashir, *J. MEMS*, 2005, **14**, 103–112.
52 P. S. Willams, T. Koch and J. C. Giddings, *Chem. Eng. Commun.*, 1992, **111**, 121–147.
53 M. Washizu and T. B. Jones, *J. Electrostat.*, 1994, **33**, 187–198.
54 T. B. Jones and M. Washizu, *J. Electrostat.*, 1996, **37**, 121–134.
55 E. L. Casternsen, R. E. Marguis and P. Gerhardt, *J. Bacteriol.*, 1971, **107**, 106–113.

